WAR Journal of Multidisciplinary Bulletin
(WARJMB)

ISSN (Online): 1595-6709
ISSN (Print): 1595-6636

Received: 25-02-2026 Revised: 03-03-2026 Accepted: 07-03-2026 Published: 09-03-2026

Research Article

Characterization of Land Surface Emissivity (LSE): a Sustainable Approach to Heat Disaster Mitigation of Minna City and Environs, Niger State, Nigeria

Adama, C. K.,
Department of Geography, Ibrahim Badamasi Babangida University, Lapai, Nigeria

OPEN ACCESS

Published in
VOI- 2 Issue: 2

DOI:10.5281/zenodo.18976996

PP: 10-17

Correspondence:

Adama, C. K.,
Department of Geography, Ibrahim Badamasi Babangida University, Lapai, Nigeria

Abstract

This study characterized the Land Surface Emissivity (LSE) as a sustainable approach to heat disaster mitigation of Minna City and Environs, Niger State, Nigeria. The study aimed to examine the spatial variation of LSE using Satellite Remote (SR) sensing and Geographic Information System (GIS) from the city center to the fringes. The study utilized satellite data retrieval and analysis which was the algorithm for extracting LST from Landsat 5, 7 and 8 thermal infrared sensors, using different surface emissivity sources from the Google Earth Engine (GEE). The LSE imageries were retrieved in 2022, 2014 and 2023 respectively. In 2002, increased LSE values were mainly detected in the rural outskirts, including areas like Gidankwanu and Maikunkele, where vegetation and water bodies were more prevalent. In contrast, the city centre showed lower LSE, due to the dominance of urban surfaces such as concrete and paved areas with limited vegetation. Over the years, the spatial distribution of LSE shifted, with higher values appearing in the eastern parts of the city by 2014, likely indicating urban greening efforts or natural plant growth. By 2023, the LSE pattern had further changed, predominantly concentrating in the northeastern region, which emphasises ongoing urban development and changes in land cover, particularly the reduction of vegetation within the city core. It is recommended that maintaining and expanding vegetative cover is a sustainable approach to mitigating UHI effects within rapidly urbanizing environments such as Minna City and environs, Niger State, Nigeria.

Keywords: Characterization, Disaster, Emissivity, Heat, Land, Mitigation, Surface

Introduction

Land Surface Emissivity (LSE) is the ratio of the amount of energy radiated on the surface of a material to that emitted from a black body at all temperatures, wavelengths, and view conditions. Land surface emissivity is a measure of the effectiveness of surface areas in cities in converting sensible heat into latent heat. It is known as the radiation of solar energy from the surface area of a material into the atmosphere [1]. In Minna town and its surroundings, there is a strong relationship between land surfaces and LST and LSE, characterized by changes in the biophysical properties under the influence of season in the area [2].

The rising amount of heat-related disasters also creates challenges to urban environments, thus calling for innovative and sustainable strategies to mitigate the effects of such disasters [3]. The importance

WAR Journal of Multidisciplinary Bulletin
(WARJMB)
ISSN (Online): 1595-6709
ISSN (Print): 1595-6636
Received: 25-02-2026 Revised: 03-03-2026 Accepted: 07-03-2026 Published: 09-03-2026

of the Earth's radiative balance, as determined by the Land Surface Emissivity (LSE), has been widely recognized as a vital parameter in understanding the Earth's surface-atmosphere interaction, especially in urban and semi-urban environments [4]. The importance of understanding the LSE has been attributed to the better understanding of the dynamics of the Earth's surface temperatures, which is vital in the assessment of heat stress as well as the development of effective strategies to mitigate the effects of heat in urban environments, especially as the global climate warms up [5].

In the traditional context, the mitigation of the heat disaster has been emphasized, where the focus has been on infrastructural and behavioral aspects; however, the properties of the surface, such as emissivity, have not been given proper attention or have been assumed superficially in most of the literature. The land surface emissivity varies spatially and temporally based on the land cover, moisture content and composition of the surface which affects the thermal behavior of the terrain [6]. Therefore, understanding the variations of LSE can provide valuable insights for thermal modeling with greater accuracy, which can be used for the assessment of temperature with the help of remote sensing techniques, so that strategies can be developed for the mitigation of the heat disaster with the help of LSE in a sustainable manner [7].

The recent advancements in remote sensing technologies have provided new avenues for precise measurements of LSE in different environments. These technologies allow for the uninterrupted measurement of the surface's emissivity, providing a dynamic view that can account for seasonal and anthropogenic effects on the land surfaces [8]. The application of remote sensing technologies in the measurement of LSE can contribute to the development of a sustainable urban ecosystem by limiting the ecological footprint of the development on the environment, as well as the efficient use of natural resources. This can be seen in the context of the development of a climate-smart urban ecosystem.

In this context, the present study aims to characterize the Land Surface Emissivity (LSE) of selected urban and peri-urban areas, with a focus on integrating sustainable practices into heat disaster mitigation. By leveraging advanced remote sensing techniques and ground-truthing methods, this research seeks to establish a robust framework for LSE assessment that can inform policymakers and urban planners. Ultimately, the goal is to enhance the understanding of surface thermal properties and promote sustainable strategies to reduce heat-related vulnerabilities, thereby contributing to resilient and livable urban environments in the face of ongoing climate challenges. Therefore, this study examined the spatial variation of LSE using Satellite Remote (SR) sensing and Geographic Information System (GIS) from the city center to the fringes in Minna town, Niger State, Nigeria.

Methodology

Minna city and its surrounding areas are situated between latitudes 9°32’0’’N and 9°42’0’’N, and longitudes 6°26’0’’E to 6°28’0’’E along the Greenwich Meridian. The city is segmented into two Local Government Areas: Chanchaga and Bosso (Figures 1).

WAR Journal of Multidisciplinary Bulletin
(WARJMB)
ISSN (Online): 1595-6709
ISSN (Print): 1595-6636
Received: 25-02-2026 Revised: 03-03-2026 Accepted: 07-03-2026 Published: 09-03-2026

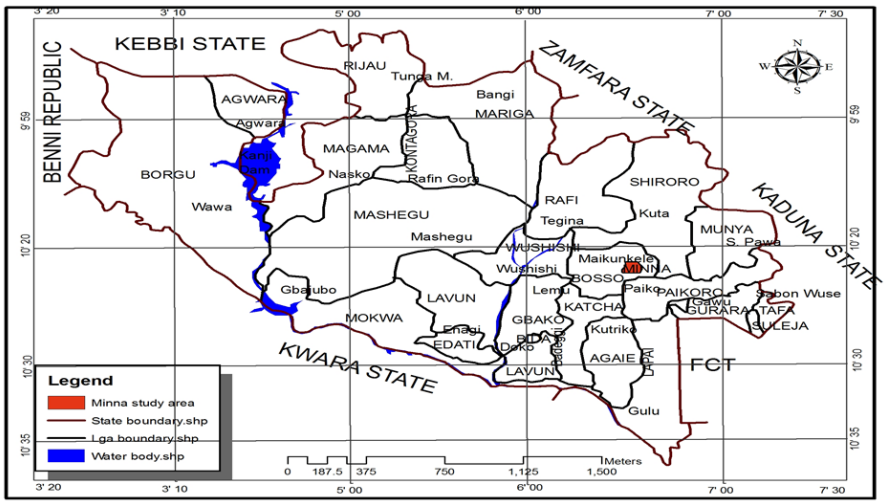

Figure 1: Minna Study Area Map

For satellite data retrieval and analysis, an algorithm for retrieving LST data from Landsat 5, 7, and 8 thermal infrared sensors using different sources of surface emissivity data from Google Earth Engine, an advanced data and analysis platform for earth sciences that allows for the estimation of LST products across any part of the globe, covering data from 2003, 2013, and 2023, has been applied.

The Landsat 5, 7, and 8 satellites have thermal infrared radiometers, thus the data were suitable for the estimation of LST. The option of using a single channel algorithm ensures the consistency of the estimated LST products, while the option of using the emissivity from different sources gives the flexibility of implementing the algorithm in any area of interest.

Out of Landsat 5, 7, and 8, only Landsat 8 has two thermal bands; therefore, the SC approach was used for consistency purposes. The Landsat 5 archive is available from March 1984 to May 2012, Landsat 7 archive is available from May 1999 to the present, while Landsat 8 archive is available from April 2013 to the present. LST products can be generated for Landsat 5, 7, and 8 satellites for the period of their operation. The SC approach describes the data used for LST estimation, which includes different sources of emissivity, implementation of the algorithm in GEE, and the accuracy of the products. Instant access to satellite data and computing power for processing data on the same platform, without the need for downloading, is available on GEE. The data available on the platform from different sources and satellites were arranged in the form of "image collections," making it possible to combine the data and process it simultaneously.

Another one was the single channel (SC) algorithm for the analysis of the thermal infrared data from Landsat 5, 7, and 8. The LST estimation process was carried out in the background on the Google cloud computing servers with direct access to the GEE satellite data catalogue. By using the SC algorithm, the LST (TS) can be computed from the radiance at the sensor in one band using the radiative transfer equation in the following form:

$$B(LST) = Lsen - Lup - \tau \cdot (1-\varepsilon) \cdot Ldown\pi\, \tau \cdot \varepsilon \text{ ----------} \quad (1)$$

Where B is the Planck function, L_{sen} is the radiance-at-the-sensor, L_{up} is the thermal path radiance, L_{down} is the down welling irradiance, ε is the surface emissivity and τ is the atmospheric transmissivity. In Equation (1) the L_{up}, L_{down} and τ were established to calculate the LST. They were also heavily

WAR Journal of Multidisciplinary Bulletin
(WARJMB)
ISSN (Online): 1595-6709
ISSN (Print): 1595-6636
Received: 25-02-2026 Revised: 03-03-2026 Accepted: 07-03-2026 Published: 09-03-2026

dependent on the total water vapour in an atmospheric column (precipitable water (PW)), which was easier to determine with the use of satellite data and LST estimation.

$$LST = Y\left[{}^{1}/_{\in}.(\psi_1 . L_{sen} + \psi_2 + \psi_3)\right] + \dot{o} \quad \text{..... 2}$$

Where

$$Y = \left[\frac{C_2 . L_{sen}}{T_b^2} . \left[(\lambda^4 . L_{sen})/C_1 + {}^{1}/_{\lambda}\right]\right] - 1 \quad \text{.....3}$$

$$\dot{o} = -y . L_{sen} + Tb \quad \text{.....4}$$

$$\psi = C . \begin{Bmatrix} PW^2 \\ PW \\ 1 \end{Bmatrix} \rightarrow \begin{Bmatrix} \psi_1 \\ \psi_2 \\ \psi_3 \end{Bmatrix} \begin{Bmatrix} C_{11} & C_{12} & C_{13} \\ C_{12} & C_{22} & C_{23} \\ C_{31} & C_{32} & C_{33} \end{Bmatrix} . \begin{Bmatrix} PW_2 \\ PW \\ 1 \end{Bmatrix} \text{.....5}$$

Where Planck's constant valuec1 is 1.19104×10^8 W μm^4 m^{-2} sr^{-1} and C_2 is 14,387.7 μm K; λ is the central wavelength of the thermal band of the Landsat sensor in question; L_{sen} in W sr^{-1} m^{-2} μm^{-1}; Tb is the brightness temperature in Kelvin; **C** is the coefficients table, with c_{ij} derived by simulations using different atmospheric profiles and ψ_x is the coefficients weighted with PW.

For the Landsat Thermal Radiance-at-Sensor products, the level 1T precision ortho corrected products for each of the Landsat satellites provided by the USGS were orthorectified images of the thermal infrared radiance-at-the-sensor products. These products were available in the form of an image collection for each of the Landsat satellites in the GEE catalogue. The images in the different collections contained different digital number values, which were converted to radiance-at-the-sensor using a GEE function and scaling factors. Though the spatial resolution of the Landsat thermal bands was different, consistency was achieved among different Landsat sensors because all the products were resampled to 30 m x 30 m by the USGS, using a cubic convolution resampling method.

The brightness temperature was estimated by direct inversion of the Planck function, and the GEE catalogue offers an image collection of Landsat top of the atmosphere (TOA) brightness temperature. The Landsat brightness temperature product offered by the GEE catalogue includes cloud cover information, which is derived by the Fmask algorithm. The Fmask algorithm is used for the detection of, among other things, clouds, cloud shadows, and water surfaces in Landsat imagery. The brightness temperature, as well as the information on clouds, cloud shadows, and water surfaces, is used for image collections. Landsat surface reflectance is available in the form of image collections through the GEE catalogue. The red and near-infrared bands of the Landsat imagery are used for the calculation of NDVI, which is necessary for the estimation of NDVI-based emissivity.

Emissivity is one of the important variables for LST estimation, as even small uncertainties associated with emissivity (1%) may cause significant LST errors, which can be as high as 1 K, depending on the sensor's setting, climatic conditions, and geographical location of the area of interest. Three emissivity sources were used: ASTER and MODIS emissivity, which were available within the GEE catalogue, and NDVI-based emissivity derived from Landsat red and NIR data. The rationale for employing different emissivity data lay in the opportunity to explore the advantages and disadvantages of emissivity data, comparing their influence on LST estimation for different types of land, which corresponds to different landscapes and ecosystems.

NDVI-based emissivity was estimated from the Landsat visible and near-infrared bands and typical emissivity values. The fraction of vegetation cover (FVC) was estimated using Equation (6), by

WAR Journal of Multidisciplinary Bulletin
(WARJMB)
ISSN (Online): 1595-6709
ISSN (Print): 1595-6636
Received: 25-02-2026 Revised: 03-03-2026 Accepted: 07-03-2026 Published: 09-03-2026

assuming the NDVI threshold for non-vegetated ($NDVI_{nonveg}$) and vegetated ($NDVI_{veg}$) surfaces to be 0.18 and 0.85, respectively. Emissivity was estimated using Equation (7), assuming a reference emissivity for non-vegetated (ε_{nonveg}) and vegetated surfaces (ε_{veg}) to be 0.97 and 0.99, respectively. The NDVI-based emissivity product was of 30m × 30m spatial resolution, matching exactly the Landsat thermal data.

$$FVC = \left[\frac{NDVI - NDVI_{nonveg}}{NDVI_{veg} - NDVI_{nonveg}}\right]2 \quad \ldots\ldots\ldots\ldots\ldots\ldots\ldots\ldots\ 6$$

$$\in = \in_{nonveg} . \ (1 - FVC) + \in_{veg} . FVC \quad \ldots\ldots\ldots\ldots\ldots\ldots\ 7$$

Also, algorithm for extracting LST from Landsat ETM+ data was applied in 2017 satellite data analysis where digital Number was converted to Spectral Radiance; and Spectral Radiance was adapted to at-Sensor Temperature and Emissivity. Finally, Emissivity was used to establish ST from brightness temperature value in the thermal band image of Landsat 8, band 10 and 11. Finally, analysis of NDVI was performed with the formula:

NDVI = (NIR-RED) / (NIR+RED) ---------- (8)

Where RED and NIR equals to spectral reflectance measurements acquired in red (visible) and near-infrared regions which take the values between 0.0 and that of 1.0; also this formula goes with a value that ranges from -1 as water to +1 indicating strongest vegetative growth respectively. The NDBI analysis took place with the formula thus:

NDBI = (SWIR-NIR) / (SWIR + NIR) ---------- (9)

Where the Sun elevation value = 51.8851 and the Sin (sun elevation) = 0.7867748

The raster calculator was adopted to derive the output data for RED reflective and for Red band to show reflectance value within the band, NIR reflectance and finally the SWIR reflectance.

Landsat 5, 7 and 8 thermal infrared sensors, using different surface emissivity sources from the Google Earth Engine (GEE) and Landsat ETM+ were engaged to achieve the changes in LST and LSE. The NDVI and NDBI were used to understand changes in vegetal cover and built-up areas. The NDVI was to create the differences in land greenness. The NDBI clearly separates built-up parcels by grouping infrastructure and pavement materials.

Results and Discussion

Figure 2 showed the Land Surface Emissivity (LSE) of Minna town and environs in 2002. It revealed that there was high LSE concentration in the surrounding (rural outskirt) of the city such as Kwana, Gidankwanu, Maikunkele, Taige, etc. In this year (2002), the city centre recorded low LSE due to poor vegetal cover such as Mobile, Kpakungu and City Gate areas respectively. Figure 3 revealed the Land Surface Emissivity (LSE) of Minna town and environs in 2014. The imagery showed that LSE concentrated more in the eastern part of the city due to increased vegetal cover with its low appearance at the city centre. Figure 4 revealed the Land Surface Emissivity (LSE) of Minna town and environs in 2023. The pattern of LSE unveiled that it concentrated in the north eastern segment. This emphasized the result that LSE decreased from the rural fringes to the city centre due to variation in the density of vegetation and urban pavement materials.

Accordingly, vegetation and water bodies have more emissivity values than urban materials. This is in tandem with [10] who studied emissivity of crop plants such as mature Phalaenopsis, Paphiopedilum,

WAR Journal of Multidisciplinary Bulletin
(WARJMB)
ISSN (Online): 1595-6709
ISSN (Print): 1595-6636
Received: 25-02-2026 Revised: 03-03-2026 Accepted: 07-03-2026 Published: 09-03-2026

Malabar and chestnut recording the values of 0.9809, 0.9783, 0.981 and 0.9848 respectively. Sand, water and green grass have emissivity values of 0.949 - 0.962, 0.993 - 0.998 and 0.975 - 0.986 compared to the low emissivity of urban materials such as concretes 0.95-0.97, cement 0.54, gravel 0.28, bricks 0.90-0.94, asbestos 0.96 and aluminum 0.05-0.77 respectively [11]. In this vein, emissivity is higher at the rural fringes than the inner city as plants and water bodies at the fringes quickly use energy for evapotranspiration, and free the energy in them thereby keeping the rural fringes cool. Thus, UHI is expected to concentrate on the inner city than the rural fringes. Similarly, UHI increases from rural fringes to the city center and emissivity decreases from rural fringes to the city center due to differences in urban materials, water bodies and vegetal cover between the city center and the rural outskirts.

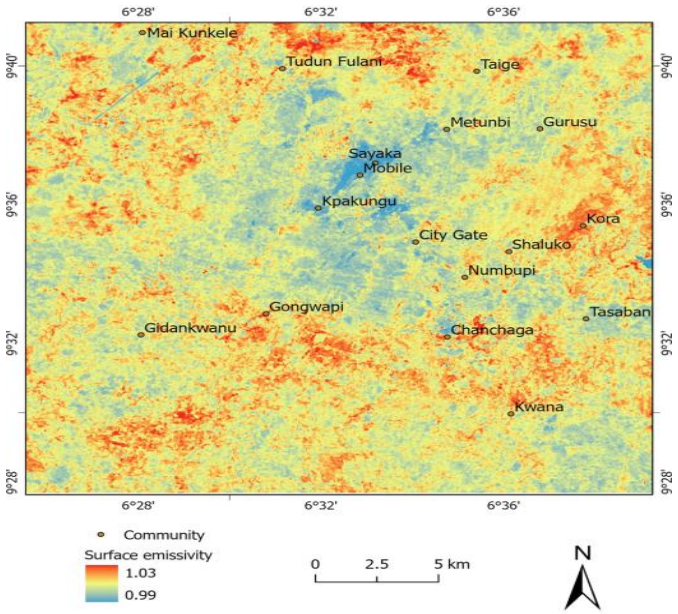

Figure 2: Land Surface Emissivity (LSE) of Minna Town and Environs (2002)

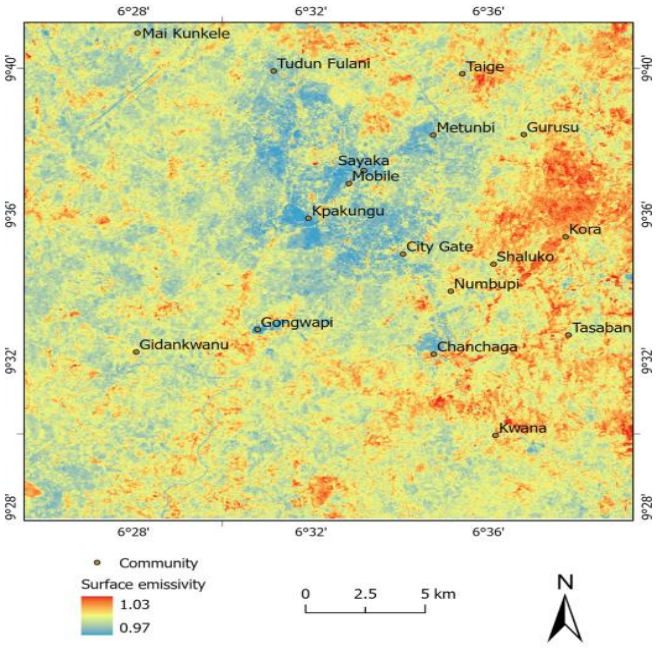

Figure 3: Land Surface Emissivity (LSE) of Minna Town and Environs (2014)

WAR Journal of Multidisciplinary Bulletin
(WARJMB)
ISSN (Online): 1595-6709
ISSN (Print): 1595-6636
Received: 25-02-2026 Revised: 03-03-2026 Accepted: 07-03-2026 Published: 09-03-2026

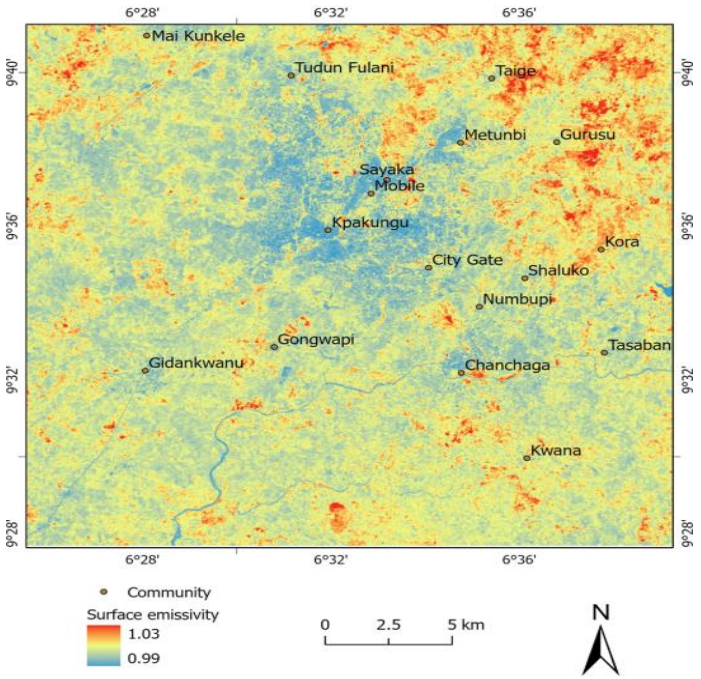

Figure 4: Land Surface Emissivity (LSE) of Minna Town and Environs (2023)

Conclusion

The results from the three temporal epochs, that is, 2002, 2014, and 2023, consistently reveal a spatial variation in Land Surface Emissivity (LSE) in Minna town and its surroundings. In the year 2002, higher values of LSE were observed in the rural outskirts, such as Gidankwanu and Maikunkele, where there was higher presence of vegetation and water bodies, while lower values were observed in the city center, where there was higher presence of surfaces such as concrete and asphalt, with minimal vegetation cover. However, in the year 2014, the spatial distribution of LSE was altered, with a higher value observed in the eastern part of the city, possibly because of the greening of the city or the growth of vegetation in the area. The spatial distribution of LSE in the year 2023 was further altered, with a higher value observed in the northeastern part, possibly because of the growth and expansion of the city, and a decrease in the amount of vegetative cover in the city center.

These results further confirm the existing relationship between different land cover types and their respective emissivity values, with higher values of emissivity observed over vegetated and water surfaces than urban surfaces. The presence of vegetation plays an active role in increasing emissivity values by evapotranspiration, which helps to retain cooler rural fringes by dissipating heat. Impervious surfaces such as concrete, bricks, and asphalt, which have lower emissivity values, contribute to retaining heat and thus create urban heat islands. The observed trend of decreasing emissivity values moving towards the urban core from the rural fringes can be attributed to an increase in impervious surfaces and a decrease in vegetative cover, resulting in higher surface temperatures. This study, therefore, recommends the significance of vegetative cover as a sustainable solution for mitigating urban heat islands.

References

1. Cheng, J & liang, S. (2017). Land-Surface Emissivity. Comprehensive Remote sensing: Earth energy budget, 217-263. Elsevier. Doi:10.1016/B978-0-12-409548-9.10374-4.

ISSN (Online): 1595-6709
ISSN (Print): 1595-6636
Received: 25-02-2026 Revised: 03-03-2026 Accepted: 07-03-2026 Published: 09-03-2026

2. Alademomi, A.S., Okolie, C.J. & Daramola, O.E. (2022). The interrelationship between LST, NDVI, NDBI, and land cover change in a section of Lagos metropolis, Nigeria. *Appl Geomat,* 14, 299–314. https://doi.org/10.1007/s12518-022-00434-2.
3. Luo, Y., Cheng, X. & He, B. J. (2025). Identification and assessment of heat disaster risk: a comprehensive framework based on hazard, exposure, adaptation and vulnerability. *Int. J. Environ. Sci. Technol.* 22, 11275–11294. https://doi.org/10.1007/s13762-024-06195-2.
4. Wang, L., Yue, P., Yang, Y., Sha, S., Hu, D., Ren, X., Wang, X., Han, H., & Jiang, X. (2025). Land Surface Condition-Driven Emissivity Variation and Its Impact on Diurnal Land Surface Temperature Retrieval Uncertainty. *Remote Sensing*, *17*(14), 2353. https://doi.org/10.3390/rs17142353.
5. Gangani, D. A. O. Waduge, M. B., Upaka, R. & Meddage, D. P. (2024). Adapting cities to the surge: A comprehensive review of climate-induced urban flooding. *Results in Engineering,* 22, 102123. https://doi.org/10.1016/j.rineng.2024.102123.
6. Srivastava, V. T., Sharma, A. & Jadon, S. S. (2026). A review of the formation, mitigation strategies from 50 years of global urban heat island studies. *Environ Dev Sustain,* 28, 97–114. https://doi.org/10.1007/s10668-024-04966-y.
7. Zhong, X., Zhao, L., Ren, P., Wang, J., Li, Y., Zhang, X., & Luo, C. (2024). Land surface emissivity retrieval from SDGSAT-1: comparison of LSE products with different spatial resolutions. *International Journal of Digital Earth*, 17(1). https://doi.org/10.1080/17538947.2023.2297940.
8. Kazanskiy, N., Khabibullin, R., Nikonorov, A., & Khonina, S. (2025). A Comprehensive Review of Remote Sensing and Artificial Intelligence Integration: Advances, Applications, and Challenges. *Sensors*, *25*(19), 5965. https://doi.org/10.3390/s25195965.
9. Paheding, S., Saleem, A. & Siddiqui, M. F. H. (2024). Advancing horizons in remote sensing: a comprehensive survey of deep learning models and applications in image classification and beyond. *Neural Comput & Applic,* 36, 16727–16767. https://doi.org/10.1007/s00521-024-10165-7.
10. Robert, H. (2015). Determining the Leaf Emissivity of Three Crops by Infrared Thermometry. doi:10.3390/s150511387.
11. Electronic Temperature Instrument [ETI] (2018). Emissivity Table. https://thermometer.co.uk/img/documents/emissivity_table.pdf.